RYERSON'S COPY

jpl INTEROFFICE MEMO

3555-76-031

DATE Nov. 8, 1976

TO Robert E. Covey SEC. 365

FROM H. McGinness *Hdm* EXT. 6081 SEC. 355

SUBJECT Dynamic Analysis of 3m Mauna Kea Telescope

Attached is the report on the subject matter. It consists of a description of the analysis, performance curves, and four appendices.

HMG:lce

cc: J. Garba
M. Gayman
R. Levy
H. Phillips
G. Smith (University of Hawaii, Institute of Astronomy)
F. Stoller
R. Wallace

A PRELIMINARY DYNAMIC ANALYSIS OF THE
3M MAUNA KEA TELESCOPE

Objective

The objective of this investigation of the 3m Mauna Kea telescope was to determine whether its transient response to a commanded hour angle (H.A.) step function would be affected significantly by the stiffness of the site soil.

The Dynamic Model

A review of the stiffness and inertia analyses of the design suggested that a discrete parameter model composed of five rotary inertias, four torsional springs, and six rotary viscous dampers would be adequate for approximating H.A. axis dynamic response. This five rotational degree of freedom model is shown in Figure 1. The entire concrete foundation is lumped into one inertia, J_1, which is attached to the ground through a soil spring, k_{01}, and a viscous damper, b_{01}. The south pier is combined with the drive motor stators and reduction gear cases to form inertia J_2 which is connected to the foundation by a spring k_{12}, representing the stiffness of the south pier, and by the damper b_{12}. The drive motor rotors and small gears of the reduction units are referenced to the H.A. axis and combined to form inertia J_3 which is connected to J_2 by the damper b_{23} and connected to J_4 by damper b_{34} and spring k_{34}. The inertia J_4 represents the combination of the telescope yoke, tube, and H.A. bullgear. The spring k_{34} represents the stiffness of the drive gears, properly referenced to the H.A. axis, combined in series with the yoke stiffness. The north pier is represented by inertia J_5 which is connected to the foundation, J_1, by the spring k_{51}, representing the north pier stiffness, and by the damper b_{15}. Inertias J_4 and J_5 are connected to each other by the viscous damper

b_{45} and by an acceleration device "a" which produces an equal and opposite torque on inertias J_4 and J_5 such that the torque magnitude is proportional to the difference in acceleration between J_4 and J_5.

John Garba of JPL Section 354 used the results of previous structural analyses to compute the inertia and spring values (Ref. 1) of most of the components of the model of Figure 1. The motor inertia and gear springs were appropriately referenced to the H.A. axis and properly included in the total values of inertias and stiffnesses as are set out in Table I. This table also lists the damping coefficients, that is, the values of the various b's employed. The derivation of the damping coefficients is given in Appendix 1.

The Servo Analysis Model

A servo system analysis was made for the configuration shown in Figure 1 which represents the dynamic model, a closed rate loop, and a closed position loop. The position loop includes the equalization network shown between the two summation junctions. The encoder of the position loop is an incremental unit geared to rotate 180 turns for each turn of the telescope H.A. axis. Each turn of the encoder yields 2^{17} binary bits. This is used with an up-down counter having a total range of zero to 64 counts, such that ± 32 counts corresponds to ± 5 volts. The sensitivity when referenced to the H.A. axis is: 45×10^6

$$(1) \quad C_4 = \frac{5}{32} \frac{180}{2\pi} 2^{17} = .586 \times 10^6 \text{ VOLT/RADIAN}$$

The rate loop tachometer shafts are attached to the drive motors. These tachometers are Inland model TG5714C with a sensitivity of 13 volts per radian per second. When referenced to the H.A. axis the effective sensitivity for the two units is:

$$(2) \quad C_3 = 2(13)144 = .00374 \times 10^6 \text{ VOLT SEC./RADIAN}$$

?

The drive motors are Inland DC Torque Motor model T-12008. It is assumed that the motor torque, L_M, is:

$$(3) \quad L_M = k_M e - m_M \dot{\theta}_M$$

where e is the voltage across the motor

$\dot{\theta}_M$ is the motor speed

k_M and m_M are constants

The Inland Catalog gives a peak torque of 2400 inch pounds at 28.5 volts. The no load speed is given as 9.3 radians per second. If the peak torque is assumed to be at zero speed, equation (3) yields the following value for k_M:

$$(4) \quad k_M = \frac{2400}{28.5} = 84.21 \text{ INCH LB./VOLT}$$

$$(5) \quad L_M = 84.21\, e - m_M \dot{\theta}_M$$

When the speed is 9.3, $L_M = 0$, and the peak voltage is assumed to be 28.5. For these conditions equasion (5) yields:

$$(6) \quad m_M = \frac{84.21\,(28.5)}{9.3} = 258 \text{ INCH LB. SEC.}$$

Page 275 of Reference 2 suggests that m_M be taken as follows:

$$(7) \quad m_M = 1/2 \, \frac{\text{STALL TORQUE}}{\text{NO LOAD SPEED}}$$

In this way the value of k_M is half that given by equation (6), namely 129. Using this value equation (5) becomes:

$$(8) \quad L_M = 84.21\, e - 129\, \dot{\theta}_M$$

There are two drive motors torqued against each other to prevent backlash. The gear ratio between motor and telescope H.A. axis is 144. The total torque, L_T when referenced to the H.A. axis is:

$$(9)^* \quad L = 2\,(144)\left[84.21\, e - 129\, \dot{\theta}_M\right]$$

$$(10) \quad \dot{\theta}_M = 144\, \dot{\theta}_T = 144\,(\dot{\theta}_3 - \dot{\theta}_2)$$

Substituting (10) into (9) yields:

$$(11)\quad L = 24252\, e - 5\,349\,888\,(\dot{\theta}_3 - \dot{\theta}_2)$$

where e is the voltage across one motor

L is torque in inch pounds

$\dot{\theta}_3$ and $\dot{\theta}_2$ are respectively the angular velocities of the H.A. axis motor rotor and stator.

The coefficients of (11) are the values of k_1 and m used in the analysis, that is,

k_1 = .02425 10^6 INCH LB./VOLT

m = 5.35 10^6 INCH LB. SECOND

*It is, of course, assumed that the preload values of the motors are small enough to give sense to the factor of 2 in equation (9), and large enough to prevent backlash.

Equations of Motion

By referring to Figure 1 the equations of dynamic equilibrium may be written as follows:

(21) $$J_1\ddot{\theta}_1 = -k_{01}\theta_1 - k_{12}(\theta_1-\theta_2) - k_{51}(\theta_1-\theta_5) - b_{01}\dot{\theta}_1 - b_{12}(\dot{\theta}_1-\dot{\theta}_2) - b_{15}(\dot{\theta}_1-\dot{\theta}_5)$$

(22) $$J_2\ddot{\theta}_2 = -k_{12}(\theta_2-\theta_1) - b_{12}(\dot{\theta}_2-\dot{\theta}_1) - b_{23}(\dot{\theta}_2-\dot{\theta}_3) - L$$

(23) $$J_3\ddot{\theta}_3 = -k_{34}(\theta_3-\theta_4) - b_{23}(\dot{\theta}_3-\dot{\theta}_2) - b_{34}(\dot{\theta}_3-\dot{\theta}_4) + L$$

(24) $$J_4\ddot{\theta}_4 = -k_{34}(\theta_4-\theta_3) - b_{34}(\dot{\theta}_4-\dot{\theta}_3) - b_{45}(\dot{\theta}_4-\dot{\theta}_5) + a(\ddot{\theta}_4-\ddot{\theta}_5)$$

(25) $$J_5\ddot{\theta}_5 = -k_{51}(\theta_5-\theta_1) - b_{45}(\dot{\theta}_5-\dot{\theta}_4) - b_{15}(\dot{\theta}_5-\dot{\theta}_1) - a(\ddot{\theta}_5-\ddot{\theta}_4)$$

where L is the motor torque, the θ's are the angular displacements, the b's are the viscous damping coefficients, and "a" is the coefficient of an acceleration device which produces equal and opposite torques on inertias J_4 and J_5 such that the torques are proportional to the difference of the accelerations. This coefficient is kept in the equations of motion for possible future use. However, the computed results of this report are for "a" = 0.

From equation (11) it may be seen that L has the following form:

(26) $$L = k_1 e - m(\dot{\theta}_3 - \dot{\theta}_2)$$

where k_1 and m correspond respectively to 24252 and 5349888.

By referring to the feedback loops of Figure 1, the Laplace transform of the motor voltage, denoted as $\bar{e}$, can be expressed as follows:

(27) $$\bar{e}_{IN} = \left\{\left[C_1\bar{\pi} - C_4(\bar{\theta}_4-\bar{\theta}_2)\right]A_2\,\frac{1}{s}\,\frac{s+\alpha}{s+\beta} - C_3\,s(\bar{\theta}_3-\bar{\theta}_2)\right\}A_1$$

where $\bar{R}$ is the transform of the input r(t)

S is the complex variable of the frequency domain

A_2 and A_1 are gain factors

C_1 is a dimensional constant

α and β are network frequencies

The transform of (26) yields:

$$\bar{L} = k_1 e - ms(\bar{\theta}_3 - \bar{\theta}_2) \quad (28)$$

The substitution of (27) into (28) yields:

$$\bar{L} = C_1 A_2 A_1 k_1 \frac{1}{S} \frac{S+\alpha}{S+\beta} \bar{R} - C_4 A_2 A_1 k_1 \frac{1}{S} \frac{S+\alpha}{S+\beta} \bar{\theta}_4 + \left[C_4 A_2 A_1 k_1 \frac{1}{S} \frac{S+\alpha}{S+\beta} - (C_3 A_1 k_1 + m)\right] \bar{\theta}_3 + (C_3 A_1 k_1 + m) S \bar{\theta}_2 \quad (29)$$

The transforms of (21) through (25), with (29) substituted for $\bar{L}$ produces the following five equations of motion in the frequency domain in terms of inertia, spring constants, damping coefficients, network frequencies, and motor, tachometer, and encoder constants.

(31)

$$\left[J_1 s^2+(b_{01}+b_{12}+b_{15})s+(k_{01}+k_{12}+k_{51})\right]\bar{\theta}_1-(b_{12}s+k_{12})\bar{\theta}_2-(k_{51}+b_{15}s)\bar{\theta}_5 \qquad = 0$$

(32)

$$-(b_{12}s+k_{12})\bar{\theta}_1+\left[J_2 s^2+(b_{12}+b_{23}+m+C_3A_1k_1)s+k_{12}+C_4A_2A_1k_1\frac{1}{s}\frac{s+\alpha}{s+\beta}\right]\bar{\theta}_2-\left[(b_{23}+m+C_3A_1k_1)s\right]\bar{\theta}_3-\left[C_4A_2A_1k_1\frac{1}{s}\frac{s+\alpha}{s+\beta}\right]\bar{\theta}_4=-C_1A_2A_1k_1\frac{1}{s}\frac{s+\alpha}{s+\beta}\bar{\pi}$$

(33)

$$-\left[(b_{23}+m+C_3A_1k_1)s+C_4A_2A_1k_1\frac{1}{s}\frac{s+\alpha}{s+\beta}\right]\bar{\theta}_2+\left[J_3 s^2+(b_{23}+m+C_3A_1k_1+b_{34})s+k_{34}\right]\bar{\theta}_3+\left[C_4A_2A_1k_1\frac{1}{s}\frac{s+\alpha}{s+\beta}-k_{34}-b_{34}s\right]\bar{\theta}_4=C_1A_2A_1k_1\frac{1}{s}\frac{s+\alpha}{s+\beta}\bar{\pi}$$

(34)

$$-\left[b_{34}s+k_{34}\right]\bar{\theta}_3+\left[(J_4-a)s^2+(b_{34}+b_{45})s+k_{34}\right]\bar{\theta}_4+\left[as^2-b_{45}s\right]\bar{\theta}_5 \qquad = 0$$

(35)

$$-\left[b_{15}s+k_{51}\right]\bar{\theta}_1-\left[as^2+b_{45}s\right]\bar{\theta}_4+\left[(J_5+a)s^2+(b_{15}+b_{45})s+k_{51}\right]\bar{\theta}_5 \qquad = 0$$

From these the desired transfer functions may be obtained by sundry methods, for example, by Cramers rule. Notice that in using these for obtaining open rate loop transfer functions, the constant C_4 is to be set at zero.

Once having determined the desired stability and gains by root locus plotting, equations (31) through (35) could be solved for the desired transformed variables. Then these transformed variables could be inverted to give the solution in the time domain.

It was chosen instead to employ the transfer functions only for root locus plotting. Once the gains had been established to insure closed loop stability, suitable time domain equations of motion were used. These were derived as follows: equation (27) was rewritten so that only the term containing $\bar{\pi}$ was on the right hand side, obtaining:

$$\bar{e} + A_1A_2C_4\frac{1}{S}\frac{S+\alpha}{S+\beta}\bar{\theta}_4 - A_1A_2C_4\frac{1}{S}\frac{S+\alpha}{S+\beta}\bar{\theta}_2 + A_1C_3S\bar{\theta}_3 - A_1C_3S\bar{\theta}_2 = A_1A_2C_1\frac{1}{S}\frac{S+\alpha}{S+\beta}\bar{\pi} \qquad (36)$$

The following was obtained by the elimination of the denominator term, $S(S+\beta)$:

$$\bar{e}(S^2+\beta S) + A_1A_2C_4(S+\alpha)\bar{\theta}_4 - A_1A_2C_4(S+\alpha)\bar{\theta}_2 + A_1C_3(S^3+\beta S^2)\bar{\theta}_3 - A_1C_3(S^3+\beta S^2)\bar{\theta}_2 = A_1A_2C_1(S+\alpha)\bar{\pi} \qquad (37)$$

Equation (37) is the transform of the following time domain equation, having zero initial conditions:

$$\ddot{e} + \beta\dot{e} + A_1A_2C_4\dot{\theta}_4 + A_1A_2C_4\alpha\theta_4 - A_1A_2C_4\dot{\theta}_2 - A_1A_2C_4\alpha\theta_2 + A_1C_3\dddot{\theta}_3 + A_1C_3\beta\ddot{\theta}_3 - A_1C_3\dddot{\theta}_2 - A_1C_3\beta\ddot{\theta}_2 = A_1A_2C_1\dot{\pi} + A_1A_2C_1\alpha\pi \qquad (38)$$

The substitution of (26) into (22) and (23) yields respectively:

$$J_2\ddot{\theta}_2 = -k_{12}(\theta_2-\theta_1) - b_{12}(\dot{\theta}_2-\dot{\theta}_1) - b_{23}(\dot{\theta}_2-\dot{\theta}_3) - k_1e_{IN} + m(\dot{\theta}_3-\dot{\theta}_2) \qquad (22\ a)$$

$$J_3\ddot{\theta}_3 = -k_{34}(\theta_3-\theta_4) - b_{23}(\dot{\theta}_3-\dot{\theta}_2) - b_{34}(\dot{\theta}_3-\dot{\theta}_4) + k_1e_{IN} - m(\dot{\theta}_3-\dot{\theta}_2) \qquad (22\ b)$$

Equations (22a) and (23a) can be differentiated and respectively solved explicitly for $\dddot{\theta}_2$ and $\dddot{\theta}_3$, which when substituted into (38) reduces it to a second order equation, namely equation (46), which together with (21), (22a), (23a), (24) and (25) constitute six second order differential equations in the variables $\theta_1, \theta_2, \theta_3, \theta_4, \theta_5, e_{IN}$. The constant coefficients are functions only of the parameters of the physical system. When systematically rewritten, the six equations are as follows, where the initial conditions are all zero, and the inputs π and $\dot{\pi}$ are functions of time:

(41) $$J_1\ddot{\theta}_1+(b_{01}+b_{12}+b_{15})\dot{\theta}_1+(k_{01}+k_{12}+k_{51})\theta_1-b_{12}\dot{\theta}_2-k_{12}\theta_2-b_{15}\dot{\theta}_5-k_{51}\theta_5=0$$

(42) $$-b_{12}\dot{\theta}_1-k_{12}\theta_1+J_2\ddot{\theta}_2+(b_{12}+b_{23}+m)\dot{\theta}_2+k_{12}\theta_2-(b_{23}+m)\dot{\theta}_3+k_1 e_{IN}=0$$

(43) $$-(b_{23}+m)\dot{\theta}_2+J_3\ddot{\theta}_3+(b_{34}+b_{23}+m)\dot{\theta}_3+k_{34}\theta_3-b_{34}\dot{\theta}_4-k_{34}\theta_4-k_1 e_{IN}=0$$

(44) $$-b_{34}\dot{\theta}_3-k_{34}\theta_3+(J_4-a)\ddot{\theta}_4+(b_{34}+b_{45})\dot{\theta}_4+k_{34}\theta_4+a\ddot{\theta}_5-b_{45}\dot{\theta}_5=0$$

(45) $$-b_{15}\dot{\theta}_1-k_{51}\theta_1-a\ddot{\theta}_4-b_{45}\dot{\theta}_4+(J_5+a)\ddot{\theta}_5+(b_{45}+b_{15})\dot{\theta}_5+k_{51}\theta_5=0$$

(46) $$-\frac{A_1C_3b_{12}}{J_2}\ddot{\theta}_1-\frac{A_1C_3k_{12}}{J_2}\dot{\theta}_1+A_1C_3\left(\frac{b_{12}+b_{23}+m}{J_2}+\frac{b_{23}+m}{J_3}-\beta\right)\ddot{\theta}_2+\left(\frac{A_1C_3k_{12}}{J_2}-A_1A_2C_4\right)\dot{\theta}_2-A_1A_2C_4\alpha\theta_2+$$

$$-A_1C_3\left(\frac{b_{23}+m}{J_2}+\frac{b_{34}+b_{23}+m}{J_3}-\beta\right)\ddot{\theta}_3-\left(\frac{A_1C_3k_{34}}{J_3}\right)\dot{\theta}_3+\frac{A_1C_3b_{34}}{J_3}\ddot{\theta}_4+\left(\frac{A_1C_3k_{34}}{J_3}+A_1A_2C_4\right)\dot{\theta}_4+$$

$$+A_1A_2C_4\alpha\,\theta_4+\ddot{e}_{IN}+\left(\frac{A_1C_3k_1}{J_2}+\frac{A_1C_3k_1}{J_3}+\beta\right)\dot{e}_{IN}=A_1A_2C_1\dot{r}+A_1A_2C_1\alpha r$$

Solution of the System of Equations

The equations of motions in terms of the motor torque were first written in the time domain. The expansion of the motor torque function was Laplace transformed in order to be consistent with a given network function which was already expressed as a transfer function. Then as explained previously the equations were converted back to the time domain. For the problem at hand estimations for all coefficients of equations (41) through (46) have been described except for coefficient "a" pertaining to the acceleration damping device. For the solutions given in this report the value of "a" was taken as zero, that is, it was assumed there was no such device, because solutions were desired for this case also. Solutions have not been obtained for finite values of "a" because its estimated value has not yet been made. Notice that the inclusion of a finite constant "a" does not affect the form of the equations nor the method of solution.

The solutions of the set of equations (41) through (46) with zero initial conditions and with various forms of inputs were obtained by Roy Levy of JPL Section 355. A description of the method of solution is given in Appendix 2.

Root Locus Plots

The forward loop transfer functions were obtained from equations (31) through (35), that is, from the equations of motion in the frequency domain. Appendix 3 contains the roots locus plots from which, first, the gain A, was established for a damping ratio of .50, and second the A_2 factors established for various values of the network parameters α and β. Actually all of these root locus plots pertain to a model slightly different from that shown in Figure 1. The difference is that the dampers were connected between each inertia and ground rather than between the inertias. Also some of the closed rate loop loci pertain to the coordinate θ_3 , whereas, θ_4 is the one of primary interest. One comparison, however, viz. where the network center frequency is at one hertz, shows about the same value of gain for both cases. If additional root loci are plotted they should pertain strictly to the model of Figure 1 and to the coordinate θ_4. It should be emphasized that all the time response curves correspond exactly to the model of Figure 1.

The position loop compensation used for this analysis is a modified double integrating type with a lead ratio of ten. This type of compensation provides zero steady state tracking error and is typically used for similar applications. No attempt was made to optimize the design and only linear networks were considered. The resultant loop bandwidths and settling times are felt to be representative of the final system performance.

Time Response Solutions

Figures 2 and 3 show the time responses of the system, with both loops closed, to unit step inputs. Figure 2 pertains to a lag-lead network of center frequency 2.70 hertz (16.97 rad/sec) and having amplifier gains of A_1 = 1.644, and A_2 = 3.842 rad/sec. The three curves of this figure correspond to three different soil stiffnesses separated by factors of ten. The curve labeled standard soil pertains to the soil spring constant listed in Table I and corresponds to a soil elastic modulus of 6000 p.s.i. [See Ref. 3 (Appendix 4)] for a discussion of the soil modulus.

Since the ordinate of this family of curves is dimensionless it may be made to match any desired input. For instance, if the unit ordinate is set at 10 arc seconds of angle, each small division represents 1/10 arc second of angle, and it requires approximately 3 seconds of time for the position error to decay to 1/10 arc second of angle. A soil of 10 times the standard stiffness would allow the decay limit of 1/10 arc second to be reached in .73 seconds of time, whereas a soil of 1/10 standard stiffness would cause the decay time for 1/10 arc second to be more than 4 seconds. It is obvious that the amount of overshoot is only weakly dependent on the soil stiffness.

If the step input is 120 arc seconds of angle, each small division of ordinate corresponds to 1.2 arc seconds. The computer output indicates it takes about 5 seconds of time for the standard soil model to decay to an error of 1/10 arc second of angle.

Figure 3 pertains to a lag-lead network with a center frequency of 2.0 hertz (12.57 rad/sec), a rate loop amplifier gain of A_1 = 1.644, and two different A_2 values. For A_2 = 2.305 rad/sec, it requires 2.3 seconds of time for a .10 arc sec. step to decay to 1/10 arc second of angle. A 120 arc second step requires 4.25 seconds of time to decay to 1/10 arc second.

When A_2 is reduced to 1.650 rad/second, the response is improved. For a 10 arc second step input, it requires 1.65 seconds of time for the response to decay to 1/10 arc second. For a 120 arc second step, it requires 3.30 seconds of time to decay to 1/10 arc second of error.

Further adjustments of the lag-lead network and the integrator gain, A_2, may produce slightly better results insofar as decaying to a small error in small time is concerned. It would appear that, in any case, a large initial overshoot will occur as long as a Type II servo system is used.

A variation made on the conditions of Figure 2, was to increase the magnitude of inertia J_1, the foundation, by a factor of ten. This produced a time response closely matching the first part of the 10 X STD. soil curve, but having an ultimate frequency corresponding to the 1/10 STD soil curve. This case has a decay error of 1/10 arc second after only .88 seconds of time for a 10 arc second step input, but the decay error after 5 seconds of time is approximately .12 arc seconds for a 120 arc second input.

Wind Loading

The equations (41) through (46) can be used for other forms of telescope excitation provided some of the right hand sides are altered. For example, it is possible to estimate the response to a torsional excitation applied only to the foundation by making the right side of equation (41) such that it represents the applied torque as a function of time, and by setting the right side of equation (46) to zero.

Since the foundation of the astrodome is close to the foundation of the telescope, there might be sufficient coupling to cause trouble. An upper bound approximation to low attenuation of the wind loading is the direct application of wind torque to the telescope foundation. For this assumption the responses of the foundation coordinate θ_1 and the telescope tube coordinate θ_4 were computed.

The change in applied torque, ΔT, is:

$$(50) \qquad \Delta T = C_D S y \tfrac{1}{2} \rho \left[(V+\Delta V)^2 - V^2 \right]$$

where C_D is the drag coefficient, ≈.60

S is the projected area of astrodome, ≈ 2070 $FT.^2$

ρ is air density at MAUNA KEA, ≈.0014 $SLUGS/FT.^3$

y is the effective vertical distance from center of pressure to H.A. axis, ≈ 8 FT.

V is the wind speed in FT./SEC.

ΔV is the increment of wind speed or gust in FT./SEC.

If the bracketed term of (50) is expanded and the $(\Delta V)^2$ term ignored, there is obtained:

$$(51) \qquad \Delta T \approx C_D S y \rho (V) \Delta V \quad .$$

If the above values are used together with V = 44 FT./SEC and ΔV = 17 FT./SEC, there results:

$$(52) \qquad \Delta T = .60(2070)\,8(.0014)\,44(17) = 10\,400 \text{ FT. LB.}$$

or approximately 125000 INCH LB.

Figure 4 shows the response of the foundation and the telescope tube to this assumed torsional step input lasting for 1/2 second, that is, a gust of 17 feet per second was suddenly supperposed onto a steady wind of 44 feet per second and then was suddenly removed after 1/2 second of time. Whether the assumption of strong coupling between the astrodome and telescope foundation is extremely conservative can only be estimated by the analysis of another dynamic model.

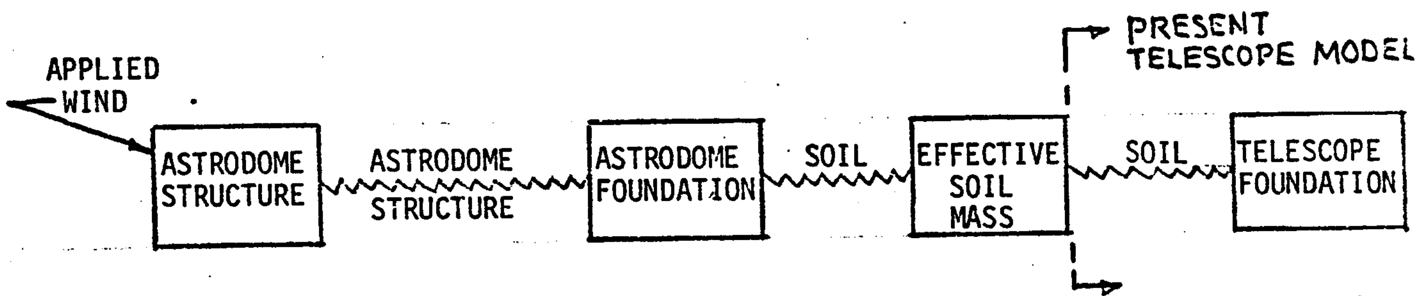

The addition of three inertias and two springs to the existing telescope model, as shown above, should be a suitable model. However, it will be difficult to evaluate the additional soil spring and effective mass, so that the final results might be widely bracketed.

Conclusions

The transient response of the telescope to a step input when controlled by a Type II servo system is significantly affected by the stiffness of the site soil when referenced to the specified performance. The desired responses cannot be achieved if the soil has an elastic modulus of 6000 p.s.i. For this modulus, the estimated response times to reach the prescribed error value of 1/10 arc second are compared to the specified times in the table below.

MAGNITUDE OF STEP INPUT IN ARC SECONDS	SPECIFIED MAX. TIME TO REACH 1/10 ARC SEC.	ESTIMATED TIME TO REACH 1/10 ARC SEC.
10	1	1.65
120	2.5	3.30

These estimated times are based upon a limited amount of network and gain combinations, however, it is believed that only slight improvements can be made in this regard.

It is recommended that further study be made of wind induced excitations.

Although not included in this report, the computer outputs are available to interested persons.

By

Houston McGinness

Robert Wallace

October 1976

References

1. JPL IOM No. 354-76-761, August 27, 1976, by John Garba
2. "Basic Feedback Control System Design" by C. J. Savant, McGraw Hill, 1958
3. JPL IOM No. 3323-75-046, March 21, 1975, by A. A. Riewe

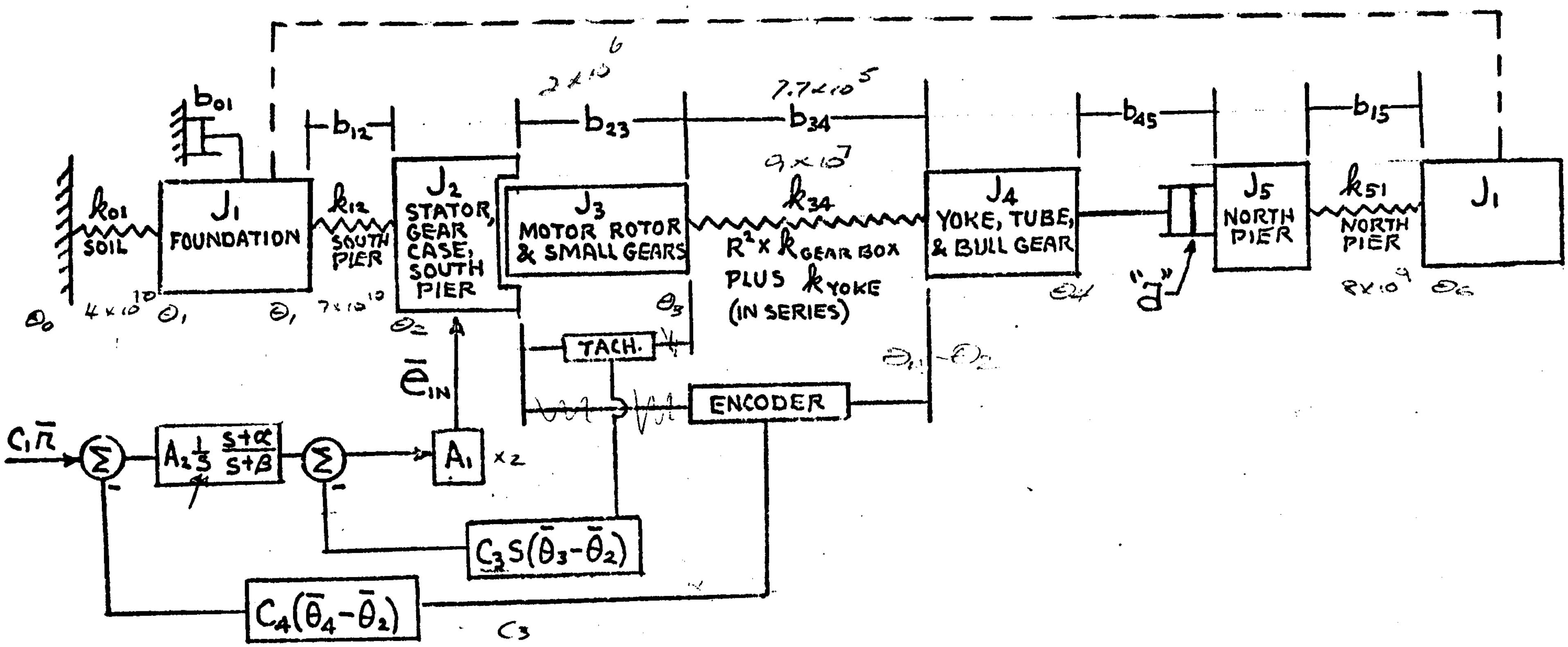

$$\bar{E}_{in} = \left[C_1\bar{\pi}_1 - C_4(\bar{\theta}_4-\bar{\theta}_2)\right] A\,\frac{1}{s}\left(\frac{s+\alpha}{s+\beta}\right) - C_3 s(\bar{\theta}_3-\bar{\theta}_2)$$

$$L = Js^2 + K(\bar{\theta}_3-\bar{\theta}_1).$$

FIG. 1, DYNAMIC MODEL OF H.A. MOTION

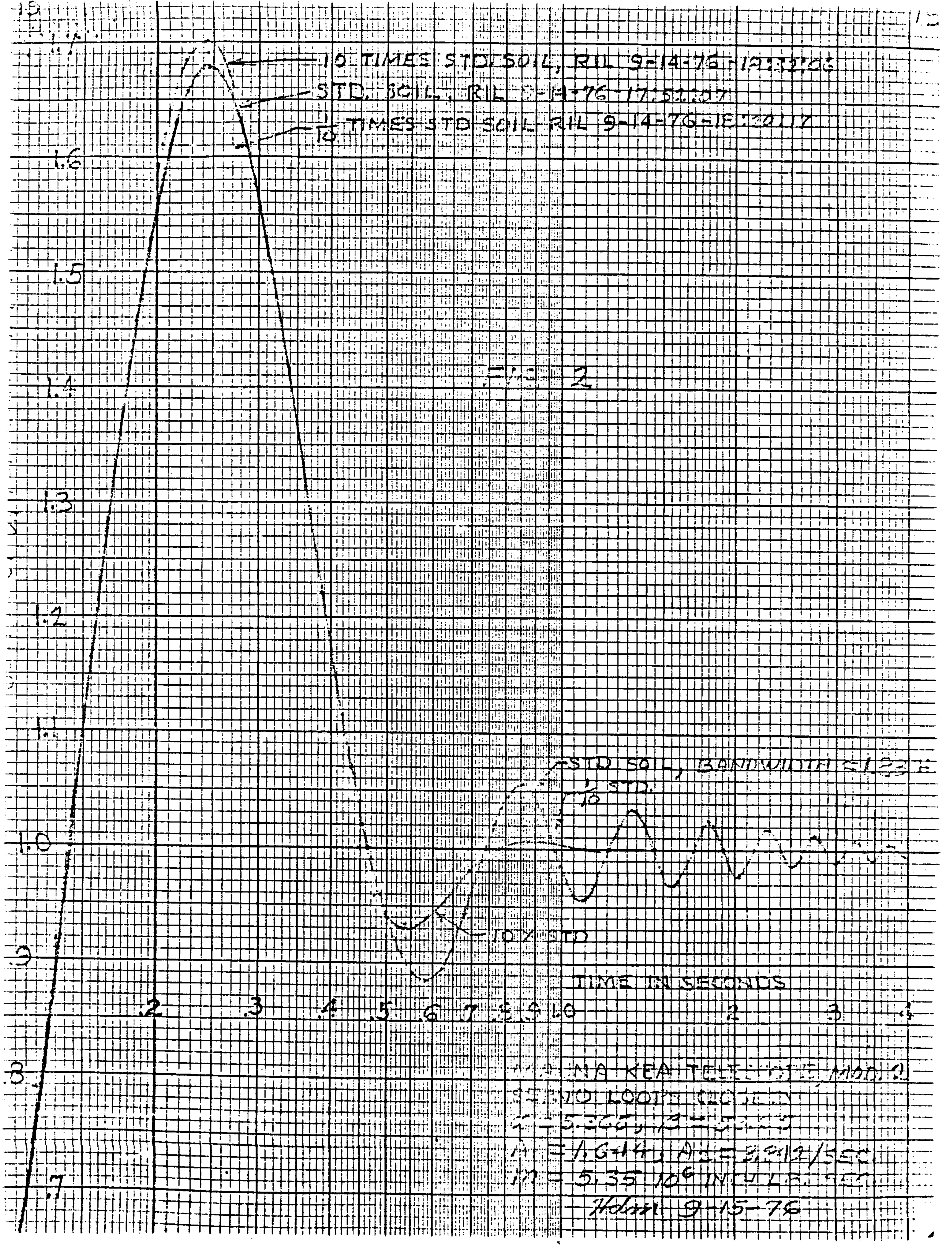
10 TIMES STD SOIL, RIL 9-14-76
STD. SOIL, RIL
1/10 TIMES STD SOIL RIL 9-14-76
1.6
1.5
1.4
1.3
1.2
1.1
1.0
.9
.8
.7
2
STD SOIL, BANDWIDTH
1/10 STD.
10 X STD
TIME IN SECONDS
.2
.3
.4
.5
.6
.7
.8
.9
1.0
2
3
4
NA KEA
LOOP
9-15-76

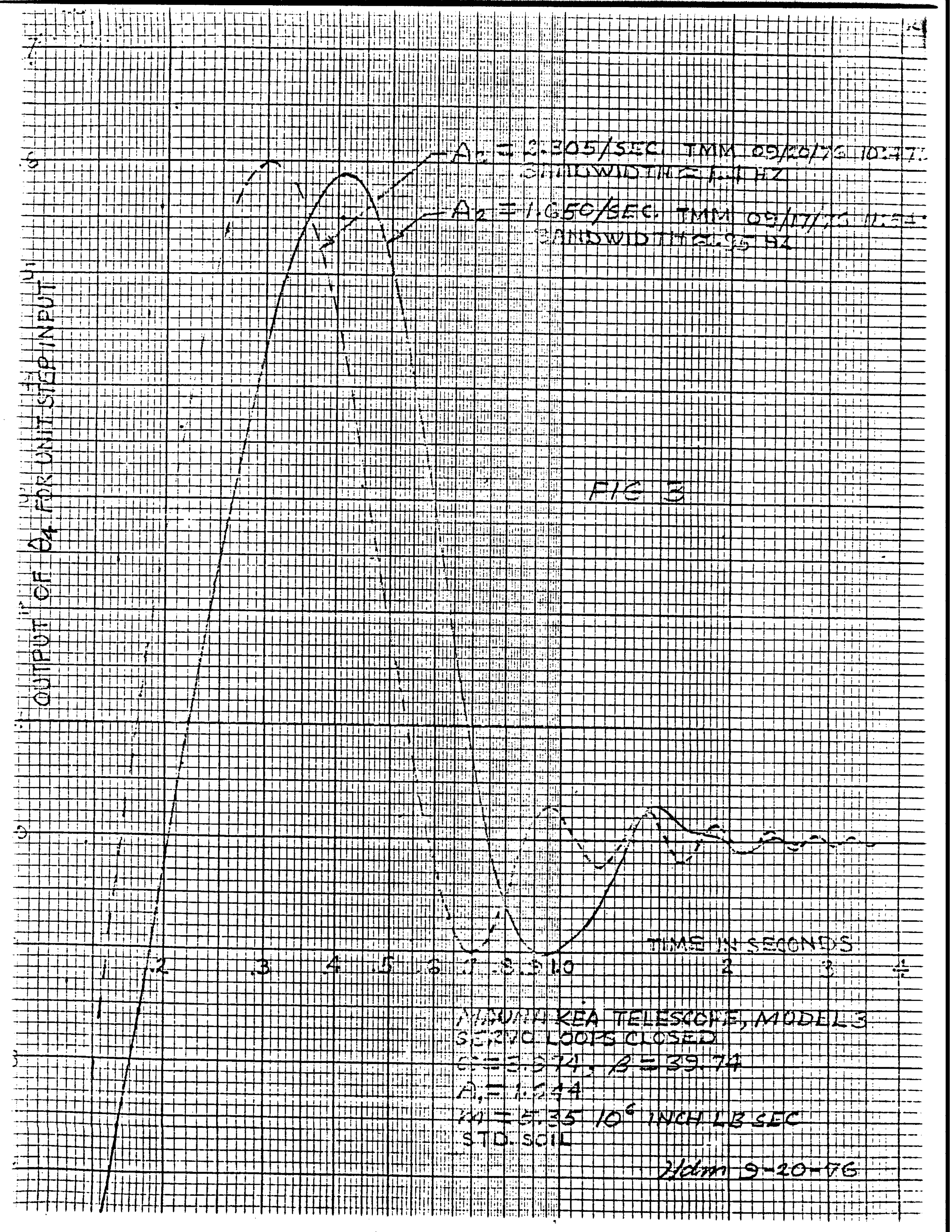
A2 = 2.305/SEC TMM 09/20/76
A2 = 1.650/SEC TMM 09/17/76
FIG 3
OUTPUT OF θ4 FOR UNIT STEP INPUT
TIME IN SECONDS
.1 .2 .3 .4 .5 .6 .7 .8 .9 1.0 2 3 4
MAUNA KEA TELESCOPE, MODEL 3
SERVO LOOPS CLOSED
β = 39.74
STD. SOIL
9-20-76

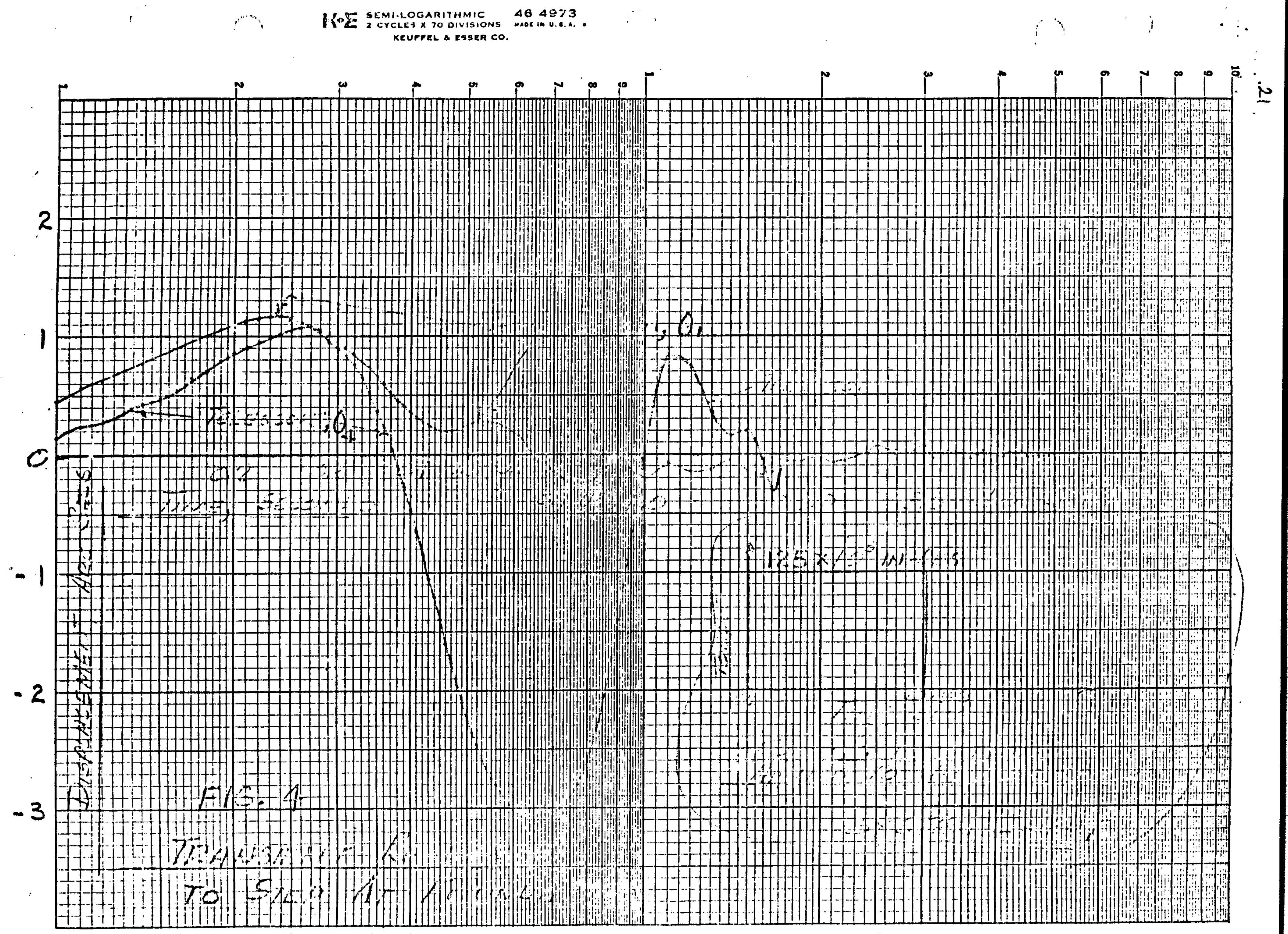

K+E SEMI-LOGARITHMIC 46 4973
2 CYCLES X 70 DIVISIONS MADE IN U.S.A.
KEUFFEL & ESSER CO.
.21
2
1
0
-1
-2
-3
FIG. 4

TABLE I

VALUES OF PARAMETERS USED

$J_1 = 219 \times 10^6$ LB. INCH SEC.^{2}
$J_2 = .0699$
$J_3 = .2888$
$J_4 = 4.715$
$J_5 = 1.50 \times 10^6$

4×10^{10}

Soil

$k_{01} = 40370 \times 10^6$ INCH LB./RADIAN FOR STD. SOIL
$k_{12} = 79600 \times 10^6$
$k_{51} = 8460 \times 10^6$
$k_{34} = 5200 \times 10^6$ — 8.8×10^7 measured
$k_c = k_{01} + k_{12} + k_{51} = 128430 \times 10^6$ FOR STD. SOIL

$b_{01} = 318 \times 10^6$ LB. INCH SEC.
$b_{12} = 1.49 \times 10^6$
$b_{15} = 2.25 \times 10^6$
$b_{23} = 2.3 \times 10^6$
$b_{34} = .775 \times 10^6$
$b_{45} = 3.3 \times 10^6$
$b_c = b_{01} + b_{12} + b_{15} = 322 \times 10^6$
$b_{23} + m = 7.65 \times 10^6$

$k_1 = .02425 \times 10^6$ INCH LB./VOLT
$m = 5.35 \times 10^6$ INCH LB. SEC.

$C_3 = .003744 \times 10^6$ VOLT ~~SEC.~~ rad
$C_4 = C_1 = .586 \times 10^6$ VOLTS/RADIAN

Appendix 1

Estimation of Damping

The damping is calculated from the viscous damping relationship:

$$b = 2\xi\sqrt{Jk} = 2\xi J\omega$$

where ξ is the damping ratio between actual and critical damping

J is the inertia

k is the spring constant

ω is the undamped frequency

The estimation is made by choosing ξ = .01 for all cases except that of the soil system where ξ was taken as .05.

When two inertias are connected by a single spring and neither is attached to other springs, the smaller inertia was used. When two inertias are connected to each other only by the damper, the smaller of the two frequencies was used. This yields the following values for the various damping coefficients, where the J and k values are from Table I, and the ω values come from the smaller of the two frequencies.

$$b_{01} = 2(.05)\sqrt{J_1 k_{01}} = 2(.05)\sqrt{219(40370)10^{12}} = 318 \; 10^6 \text{ LB.INCHS}$$

$$b_{12} = 2(.01)\sqrt{J_2 k_{12}} = 2(.01)\sqrt{.0699(79600)10^{12}} = 1.49 \; 10^6$$

$$b_{23} = 2(.01)J_3\omega_3 = 2(.01)(.288)10^6 \; 134 = 2.3 \; 10^6$$

$$b_{34} = 2(.01)\sqrt{J_3 k_{34}} = 2(.01)\sqrt{.288(5200)10^{12}} = .775 \; 10^6$$

$$b_{45} = 2(.01)J_4\omega_4 = 2(.01)(5)\,10^6 \; 33 = 3.3 \; 10^6$$

Appendix 2

Computer Solution Aids

A. Transfer Functions

The transfer function for any degree of freedom is defined as the ratio of the Laplace transforms of the response at that degree of freedom to the input. That is

$$T_j = \overline{\theta}_j/\overline{r} \qquad \text{(A-1)}$$

where $\overline{\theta}_j$ is the transform of the response at the j^{th} degree of freedom

$\overline{r}$ is the transform of the input excitation to the system

and T_j is the transfer function for the j^{th} degree of freedom

In the text, the N equations (31) through (35) are the transformed equations of motion, which can be written concisely as

$$[P]\{\overline{\theta}\} = \{\overline{V}\}\ \overline{r} \qquad \text{(A-2)}$$

in which

P is an NxN coefficient matrix of polynomials of order S^2

$\overline{\theta}$ is a N-vector of transformed response

$\overline{r}$ is the transform of the input

$\overline{V}$ is an N-vector that represents gain factors, motor parameters, and network characteristics.

Cramer's rule can be used to solve (A-2) for any of the transfer functions, which will be expressed as the ratio of two polynomials. Thus, 25

$$T_j = |P_j| \; / \; |P| \tag{A-3}$$

in which

$|P|$ is the characteristic determinant of P

and

$|P_j|$ is the determinant formed by replacing the j^{th} column of P by $\overline{V}$

The determinants in (A-3) can be expressed in factored form. For example, $|P|$ can be given as

$$|P| = \prod_{i=1}^{2N} (S - \lambda_i) \tag{A-4}$$

where λ_i is the i^{th} characteristic root (complex eigenvalue) of the matrix P.

In the case of equations (31) - (35), the numerator determinants can be simplified by factorization, which results in a reduction of order. To do this it can be observed that $\overline{V}$ is null except for the components, $\overline{u}_2$ and $\overline{u}_3$, which have the same magnitudes but opposite signs. Consequently, by adding the second row equation of (A-2) to the third row equation, the j^{th} column of $|P_j|$ will contain only the element $\overline{u}_2$. Thus, this determinant can readily be expanded by the minors of the third column. As the result

$$|P_j| = \overline{u}_2 \prod_{i-1}^{2(N-1)} (S - \lambda_{ij}) \tag{A-5}$$

in which

λ_{ij} is the i^{th} eigenvalue of the matrix formed by deleting the 2nd row and j^{th} column of P_j.

B. Computer Solution for Eigenvalues

To use standard computer software to furnish the eigenvalues for equations (A-4) and (A-5), a typical component of the coefficient matrices can be expressed as

$$p(i,j) = m(i,j)S^2 + c(i,j)\ S + k(i,j) \qquad \text{(A-6)}$$

By assembling the coefficients of like powers of S in three separate matrices, equation (A-2) can be written as

$$[M]\{S^2\bar{\theta}\} + [C]\ \{S\bar{\theta}\} + [K]\ \{\theta\} = \{\bar{V}\}\ \bar{r} \qquad \text{(A-7)}$$

where the matrices M, C, and K are of order NxN and contain the associated coefficient of the powers of S of equation (A-6).

Equation (A-7) can be put into standard eigenvalue equation form by letting

$$\{\bar{Y}\} = \begin{Bmatrix} \bar{\theta} \\ S\bar{\theta} \end{Bmatrix} \qquad \text{(A-8)}$$

$$\{S\bar{Y}\} = \begin{Bmatrix} S\bar{\theta} \\ S^2\bar{\theta} \end{Bmatrix} \qquad \text{(A-9)}$$

Then using equations (A-8) and (A-9) in (A-7) and expanding to a system of 2N equations, and considering the homogenous solution, it follows that

$$\{S\bar{Y}\} = \begin{bmatrix} [0] & [I] \\ -[M]^{-1}[K] & -[M]^{-1}[C] \end{bmatrix} \{\ \bar{Y}\ \} \qquad \text{(A-10)}$$

Transforming back in to the time domain equations (A-10) become

$$\{\dot{Y}\} = [A]\ \{Y\} \qquad \text{(A-11)}$$

where the coefficient matrix A represents the coefficient matrix of equation (A-10) and

$$\{Y\} = \begin{Bmatrix} \theta \\ \dot{\theta} \end{Bmatrix} \qquad \text{(A-12)}$$

Equation (A-11) is in standard form for use of computer library eigenvalue problem solution, which returns the roots, λ_i, $i = 1, 2, \ldots, 2N$

In writing equation (A-10), we have for convenience made the assumption that the inverse of M exists. If M is singular, the procedure is valid, but the equations may have to be recast to remove the singularity and reduce the order of the set of equations to correspond to the rank of M.

C. Solutions for Transient Response

Transient response solutions are readily developed from the foregoing. Using equations (A-11) and (A-12) and now considering the non-homogenous solutions, it follows that the transient response can be found from the solution of

$$\{\dot{Y}\} = [A]\ \{Y\} + \begin{Bmatrix} 0 \\ [M]^{-1}\{V\} \end{Bmatrix} r \qquad \text{(A-13)}$$

The above equations are a set of simultaneous first order differential equations which can be solved by almost any set of computer software packages.

The matrices M, C, K, to form the coefficient matrix A can be identified from the text equations (41)-(46) as the coefficients of the second, first and zeroth time derivatives of the θ terms, respectively. Since these equations contain both the input command and its derivative on the right had side, equation (A-13) is extended to become

$$\{\dot{Y}\} = [A]\{Y\} + \begin{Bmatrix} 0 \\ [M]^{-1}\{V1\} \end{Bmatrix} r + \begin{Bmatrix} 0 \\ [M]^{-1}\{V2\} \end{Bmatrix} \dot{r} \qquad \text{(A-14)}$$

in which V1 and V2 are the vectors associated with the command r and its derivative $\dot{r}$, respectively.

D. Computer Implementation

The computer program (RIL.TRANSMAP) reads the M, C, K matrices, initial displacement and velocity vectors, the V1 and V2 vectors and additional information required to form r and $\dot{r}$ of equation (A-14). It will optionally solve the eigenvalue problem before proceeding to the transient response solutions.

The r and $\dot{r}$ functions can be formed in several optional ways. To do this, the user supplies parameters NTYPE, VAL1, VAL2, and, VAL3. The forcing functions are automated by the program according to the following Table.

NTYPE	r	$\dot{r}$	VAL1	VAL2	VAL3
1	Sin pt	p Cos pt	p		
2	Cos pt	-p Sin pt	p		
3	step	impulse	step amplitude	start time	impulse duration time
4	ramp	constant	ramp height	start time	end time
6	rectangular pulse	impulse pair	pulse height	start time	end time
5	Tabular input for r, program interpolates and differentiates for $\dot{r}$				

Notes: 1. For NTYPE = 5 the user has to supply an additional table

2. For NTYPE = 6 the equal and opposite impulses occur at the start and end times. The duration time for impulse computation is set to the output time increment.

Additional parameters that can be supplied to direct program operations are:

N	order of the problem (must be supplied)
DELT	time increment for solution output (default = 0.1s)
TSTART	start time for solution (default = 0.0s)
TFINAL	end time for solution (default = 10.0s)
NATF	= 1, solve the eigenvalue problem, = 0 don't
NTFUNC	number of solution cases (forcing function types)
NTYPE(J), VAL1(J), VAL2(J), VAL3(J), J=1, NTFUNC	these refer to the J^{th} solution case and are as explained in the preceeding table

Required for ITYPE = 5

NTABL	number of points in input table
TIME(K),TABLE(K) K=1,NTABL	Time tags, magnitudes of r

In addition to this program there is a similar program (RIL.RESPONMAP) that operates on essentially the same matrix data. Instead of providing the transient response, the program provides the frequency response. It also solves the eigenvalue problem upon request.

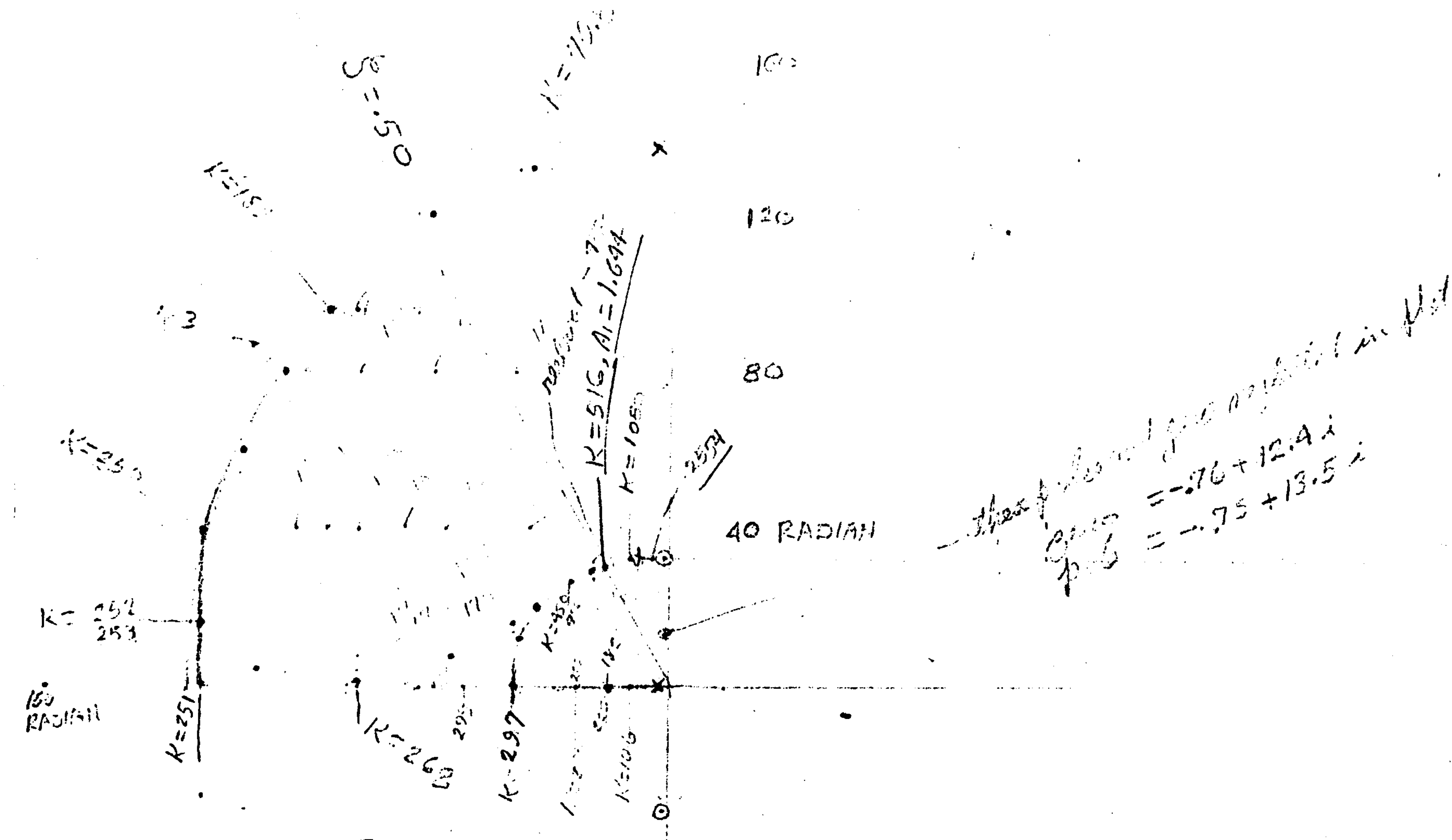

$$KGH = \left[\frac{C_3 A_1 k_1}{J_3}\right] \left[\frac{(S+.757 \pm i12.36)(S+.988 \pm i32.5)(S+2.24 \pm i75.3)(S+32.5 \pm i1069)}{(S+2.355)(S+.747 \pm i13.506)(S+2.24 \pm i75.33)(S+3.96 \pm i138)(S+32.5 \pm i1067)}\right]$$

K GH

$$KGH = \left[\frac{C_3 A_1 k}{J_3}\right] \frac{(S+1.30 \pm 43.0i)(S+1.01 \pm 31.60i)(S+2.4 \pm 75.15i)(S+32.45 \pm 1067i)}{(S+2.335)(S+1.31 \pm 4.69i)(S+2.24 \pm 75.44)(S+3.96 \pm 138.2)(S+32.4 \pm 1067i)}$$

MAUNA KEA TELESCOPE
RATE LOOP

$\bar{\theta}_x$

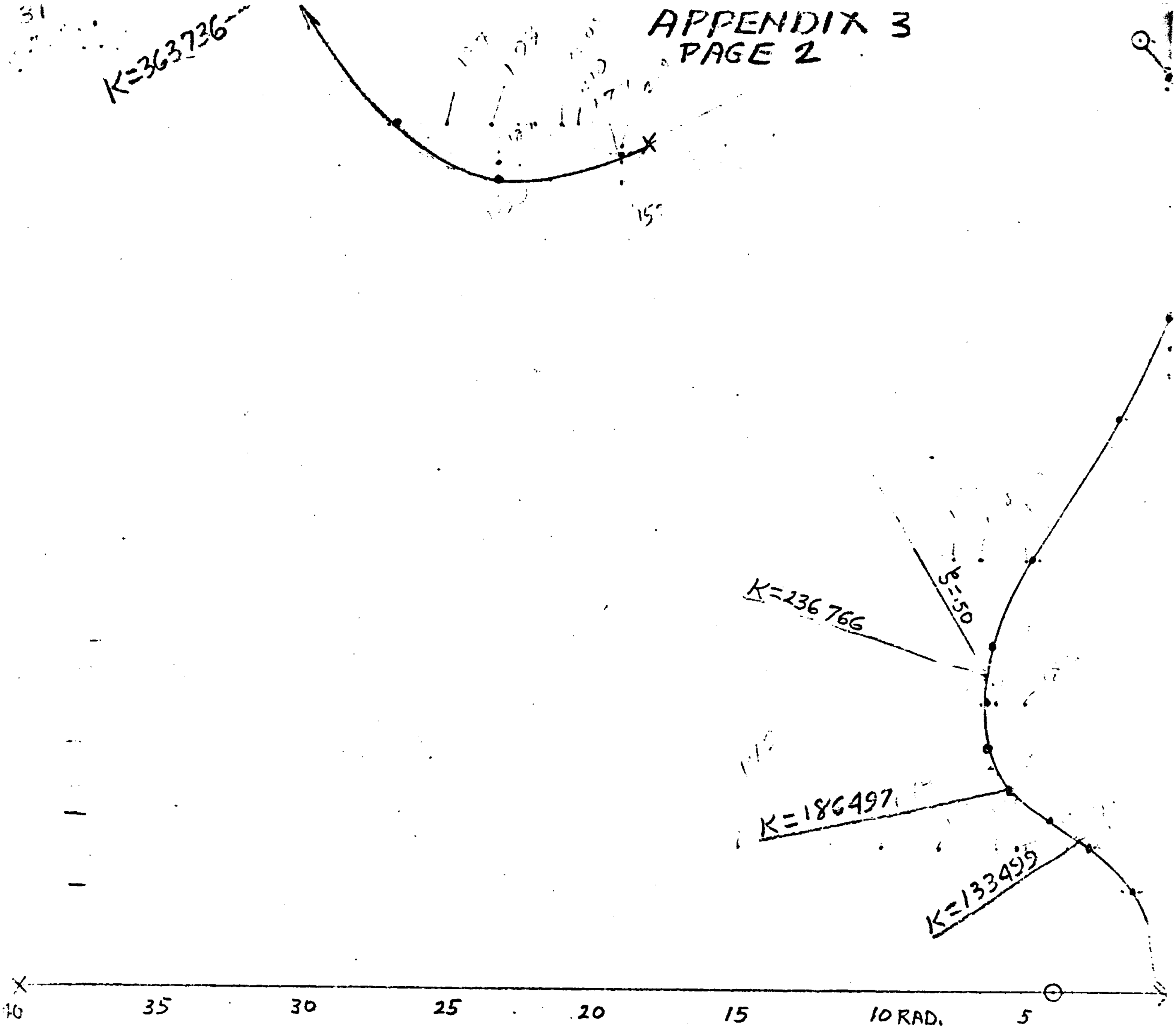

$$KGH = \left(\frac{A_2 A_1 k_1 C_4}{J_3}\right) \frac{(S+3.974)(S+.747 \pm 13.506i)(S+.996 \pm 33.194i)(S+2.24 \pm 75.33i)(S+31.96 \pm 1067)}{(S+39.738)\, S^2\, (S+2316)(S+.824 \pm 13.374i)(S+18.03 \pm 29.37i)(S+2.242 \pm 75.33i)(S+165 \pm 473)}$$

θ_3 POSITION LOOP
RATE LOOP GAIN
IS 516

₵ network at 2 Hz = 12.57
max damp ≈ .62

$$KGH = \left(\frac{A_2 F_1 \cdot k_1 C_4}{J_3}\right) \frac{(S+5.365)(S+.747 \pm 13.506i)(S+.996 \pm 33.194i)(S+2.24 \pm 75.33i)(S+31.96 \pm 1067i)}{(S+53.65)\,S^2(S+2316)(S+.824 \pm 13.374i)(S+18.08 \pm 29.37i)(S+2.242 \pm 75.33i)(S+185 \pm 473.7i)}$$

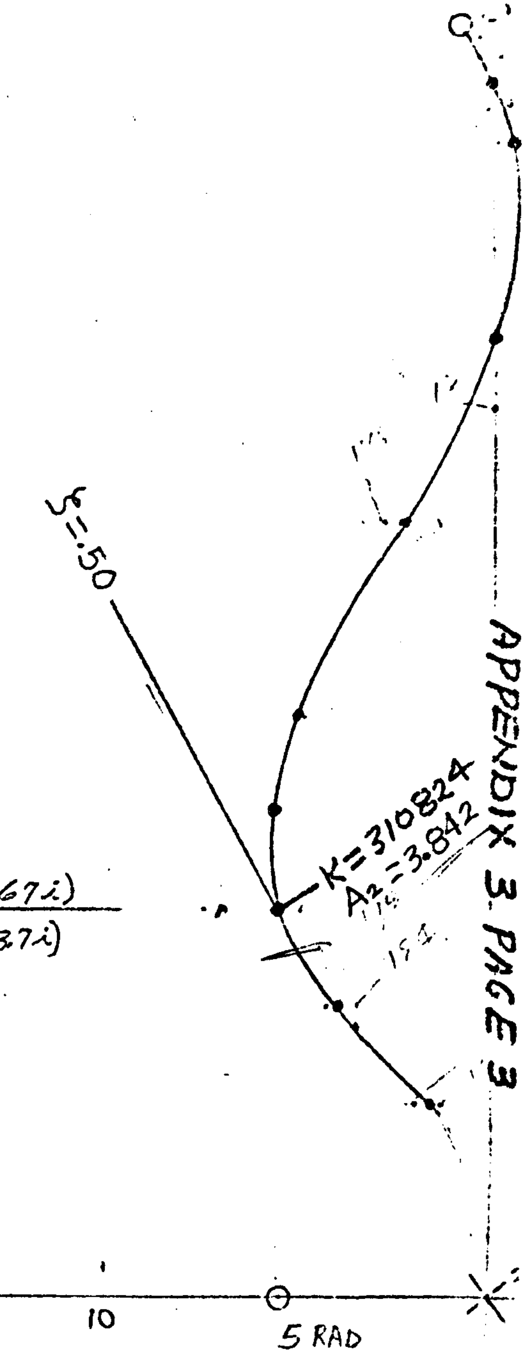

θ_3 POSITION LOOP
RATE LOOP GAIN 516
℄ NETWORK AT 2.7 HZ = 16.96 RAD.
MAX. DAMPING IS .50

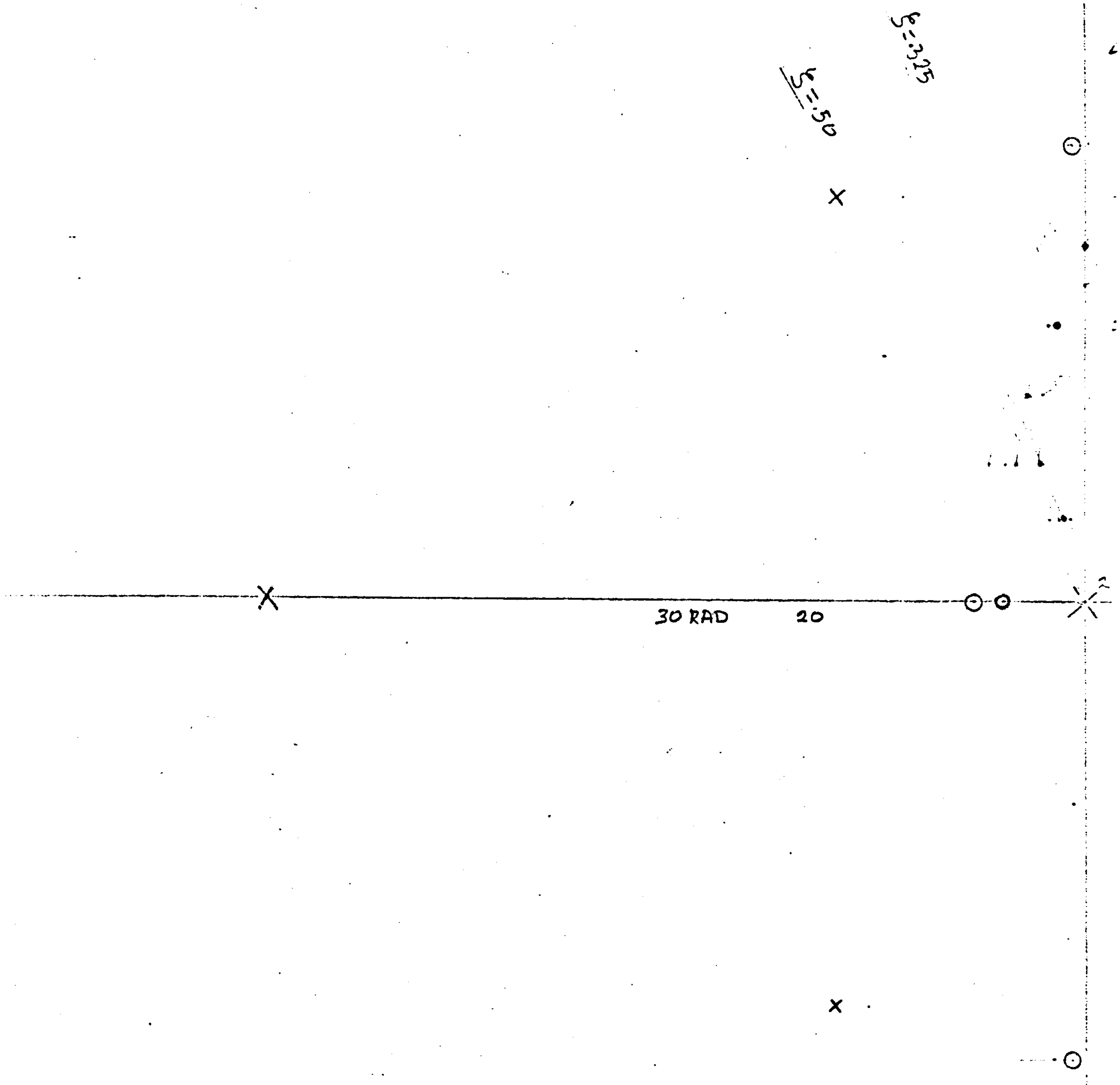

same KGH except for network

If ƒ NETWORK IS 3 HZ = 18.85 rad
DAMPING OF ABOUT .45 CAN BE ACHIEVED

SO TRY ƒ NETWORK AT 2.7 HZ

θ_3 POSITION LOOP
RATE LOOP GHIN 516 ✓
ƒ NETWORK AT 4 HZ = 25.13 RAD

MAX DAMP ≈ .325

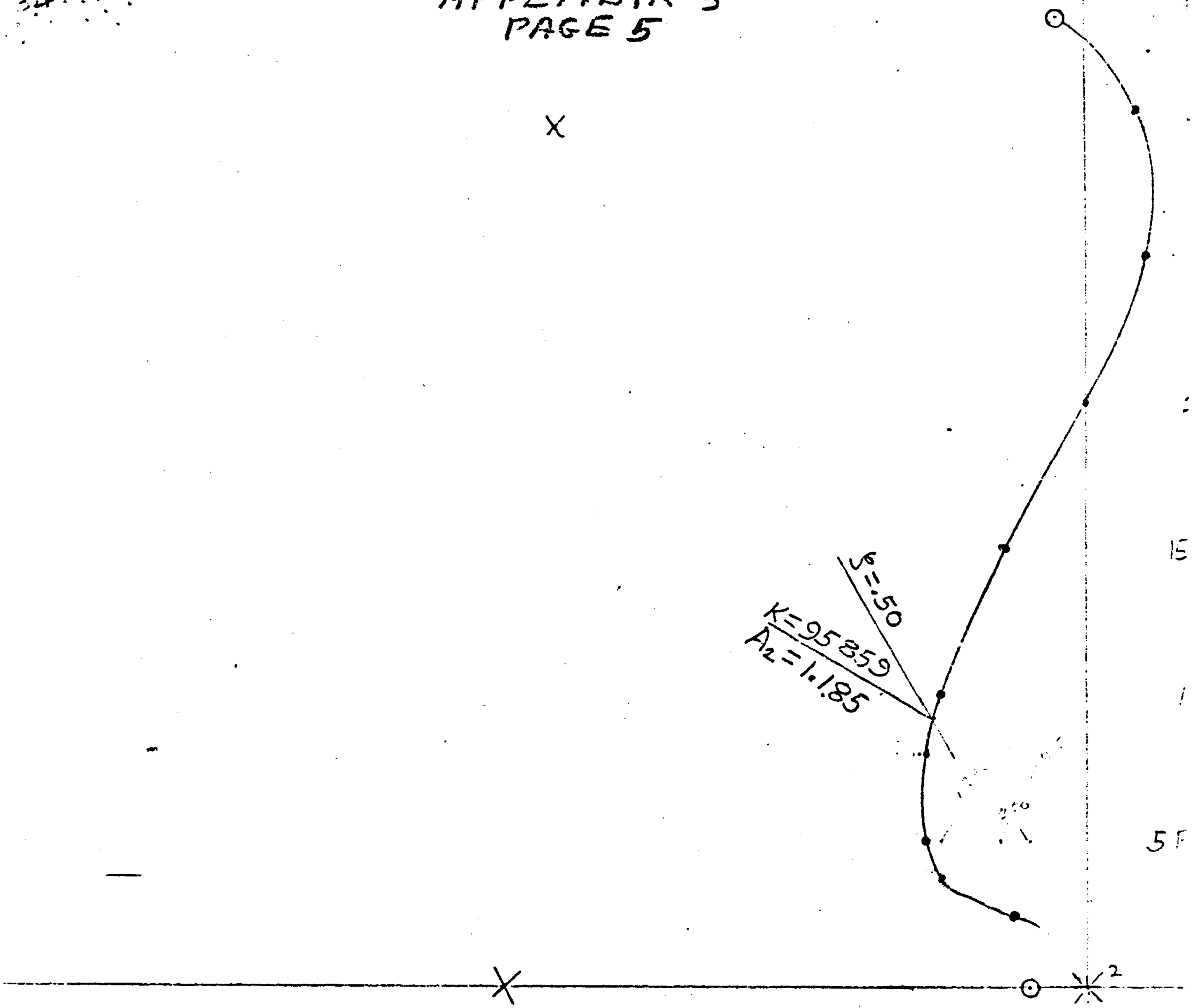

$$KGH = \frac{A_2 A_1 k_1 C_4}{J_3} \; \frac{(S+1.987)\,(S+.747 \pm 13.506i)(S+.936+33.194i)(S+2.24 \pm 25.33i)(S+31.96 \pm 1067i)}{(S+19.87)\,S^2(S+2316)(S+.824 \pm 13.374i)(S+18.08 \pm 29.37i)(S+2.242 \pm 25.33i)(S+185 \pm 473.7}$$

θ_3 POSITION LOOP
(RATE LOOP GAIN 516)

℄ NETWORK AT 1 HZ = 6.28 RAD.

max damping ≈ .83

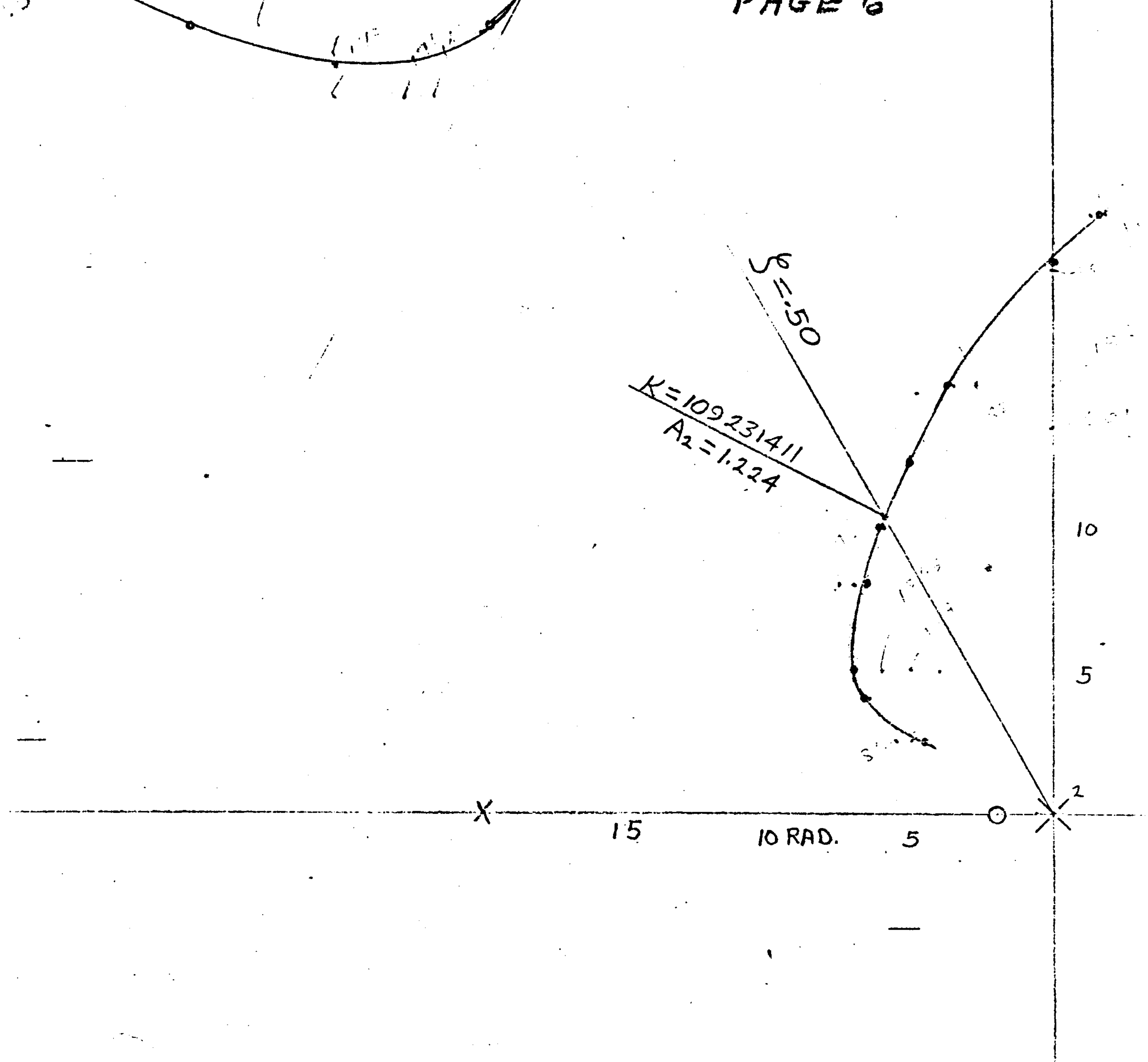

$$KGH = \frac{k_{34} A_2 A_1 k_1 C_4}{J_3 J_4} \; \frac{(S+1.087)\,(S+7.47 \pm 13.50i)\,(S+2.24 \pm 75.73i)(S+31.56 \pm 1067.)}{(S+19.87)\,S^2\,(S+23.16)(S+.824 \pm 13.74i)(S+18.08 \pm 29.37i)(S+2.242 \pm 75.73i)(S+18.5 \pm 47.7)}$$

θ_4 POSITION LOOP ✓
RATE LOOP GAIN 516
℄ NETWORK AT 1 HZ = 6.3

36 JPL → **INTEROFFICE MEMO**

APPENDIX IV PAGE 1

3323:75:046

DATE 21 March 1975

TO R. E. Covey SEC. 350

FROM → A. A. Rieve *aar* EXT. 5085 SEC. 332

SUBJECT Proposed Infra-Red Telescope - Mauna Kea, Review of Soils Data and Preliminary Drawings.

As requested comments concerning review of the subject material are submitted. Review is continuing, however, I have not as yet developed soil-spring and apparent mass factors. These will be based on the foundation configuration presented in the preliminary drawings and soil data contained in a Site Investigation and a Foundation Investigation performed for two existing observatories located in the general area of the proposed IR telescope.

It is my understanding that a complete foundation investigation, similar to those performed for the two existing observatories, will be conducted at the proposed IR telescope site in the near future.

A. Review of Foundation Investigation (Dames and Moore No. 300400111 (15903))

1. This report investigated two sites. One site was on a lava plateau at an approximate elevation of 13,000 feet and the other on the summit cinder cone at 13,700 feet. The test data and discussion concerning the summit cinder cone may be considered roughly indicative of cinder materials in other cones found subjacent to the summit cone, one of which has been selected for the proposed IR telescope. Due to sharp differences in strength and dynamic properities between lava and volcanic cinders, and in view of the extremely motion sensitive nature of the telescope, it is my opinion that the proposed observatory should be constructed on the lava materials. If it is essential to take advantage of the better sky coverage afforded by the slight additional elevation that the cinder cones offer over the lower elevation solid lava materials, measures with greater cost impact than those recommended in the Dames and Moore report will likely be required because of the very poor quality of the cinder cones. These measures will require substantial redesign of the foundation elements in order to adequately isolate the dome footings from the telescope pier footing.

   As a rough indication of the poor quality of the cinder materials notice on page 3 of the report the discussion of the "sensitivity" of cinder materials to a jeep 600 feet away whereas the lava materials were insensitive to a moving jeep at close range. As an illustration the effects of vehicular traffic at the 64 meter antenna site at Goldstone have been observed where tilts on the order of one arc second have been observed from vehicles passing within 200 feet of a test bench mounted tiltmeter. The typical soils at the Mars site are very dense, well consolidated sands and gravels of much higher quality than volcanic cinders.

2. Page 5 of Dames and Moore report presents values for Poisson's Ratio determined from the shear and compression wave velocities. The value shown for deep lava (below 70') of 0.166 is correct. The value of 0.279 indicated for the cinder cone material below 25 feet is, however, incorrect. Our computation for the cinders below 20 feet using V_c and V_s of the report yields a Poisson's Ratio of -.92 which is not valid. This is due to the poor quality of the field data which, as Dames and Moore states, is due in turn to the poor quality of the cinder materials.

3. Page 6 of the report presents the determination of Young's Modulus based on compression wave velocities. The values presented are in error because the wrong equation was used and a decimal placement error was made.

The proper equation is:

$$E = \frac{V_c^2 \rho (1 - \mu - 2\mu^2)}{g (1 - \mu)}$$

Using the following values:

<u>For Lava</u>

V_c = 2020 ft/sec

ρ = 91.5 lb/ft^3

μ = .166

<u>For Cinders</u>

V_c = 930 ft/sec

ρ = 60 lb/ft^3

μ = 0.3 (estimated)

Yields the following:

E_{lava} = 75,200 psi

$E_{cinders}$ = 8,300 psi

Due to the very poor quality of the cinder materials and the uncertainty of the dynamic field data I suggest that the above E of 8,300 psi should be reduced to something on the order of 6,000 psi. This value will be satisfactory for use in review of preliminary concepts. Final design should be based on the foundation investigation to be conducted at the actual site.

4. The conclusions presented on page 6 state that locating the observatory on cinders would be acceptable if several listed recommendations are incorporated in the design.

Recommendation No. 1 states that all vibration sources be located on lava flows at a distance approaching one mile from the observatory. This is considered highly impracticable in view of the various mechanical equipments which are required to be in close proximity to the telescope.

Recommendation No. 2 states that the profile of the observatory should be lowered to reduce the wind loads. However desirable this is, the Dames and Moore study totally neglects the critical coupling of the dome foundation deflections, as caused by wind loads, through the soil to the telescope pier foundation.

Recommendation No. 4 suggests injecting grout into the cinders around and under the structure to improve stability, but the Dames and Moore report further states there is a possibility that excessive amounts of fine materials might prevent deep penetration of grout. If this does occur what alternate corrective means are available to increase stability? None are suggested in the report and no easy corrective or alternative measures can be advanced by this writer. Further the post-construction injection of grout, as suggested by the report, is an uncertain technique which may well result in the lifting or tilting of the supported structures.

Recommendation No. 5 recommends physical separation of the building from the telescope to avoid direct transmission of wind loads to the instrument. This is highly advisable and special attention must be given to isolating all structural elements from the telescope pier and foundation. The recommendation is incomplete, however, in again neglecting the coupling action through the soil between the dome foundation and the pier as described above.

Recommendation No. 6 states that "it is believed that the response of the site to tilt from winds below 40 knots is below the estimated tolerance of 0.1 second." No supporting calculations are presented. It is my opinion that tilt of the structural elements, if founded on cinders, grouted or not grouted, will be considerably greater than 0.1 arc second. This will be investigated as part of my continuing analysis.

B. Review Comments - Dames and Moore Foundation Investigation (Job No. 9559-001-11). This report presents essentially the same basic information and recommendations contained in the earlier report reviewed under paragraph A above with additional amplifying material. The following comments are restricted to the additional material.

1. On page 3 of the report it is recommended that surface drainage be directed away from the foundation. An additional comment here is that a paved apron should be constructed about the building which extends approximately 30 feet from the building for "positive" drainage away from the observatory building area. Surface runoff from the upslope side of the observatory should be intercepted and carried around the site in lined devices to the lower side of the site. This would not be a requirement on a lava site.

2. On page 4 the use of light-weight concrete aggregate is suggested as a means to reduce transportation costs. This would appear to have merit for auxiliary structures. Use of light weight aggregates for concrete in the telescope pier and its footing would, however, be counter to the design goal of keeping the mass of the pier foundation large to obtain a low center of gravity for the overall telescope, pier and footing.

   An additional comment here is that the freeze-thaw durability of the concrete mix prepared for use in exterior sections of structures should be investigated as part of the development of the concrete mix design (ASTM tests C 290 or/and C 291). In Hawaii's warm climate this factor may have been overlooked.

3. Page 16 notes the existence of possible permafrost in the summit cone. As part of the proposed foundation investigation the ground temperatures and thermal gradients should be determined.

4. On page 24 it is suggested that dust abatement during construction could be accomplished by "heavy applications of water or low grade fuel oil." It is recommended that only water be used in light or moderate, not heavy, amounts. The use of oil is not recommended.

5. In the boring logs appended to the report the dry density values tabulated are in pounds per cubic foot not kg per cubic centimeter as indicated in the column headings.

C. Review of Preliminary Drawings

1. Drawing C803E1 prepared by C. W. Jones presents a center of gravity for the telescope, pier and footing slab which neglects the weight of backfill over the foundation slab. This should be included. Further, the c.g. of the telescope, pier and footing should be centered on the footing slab.

2. The cost estimate presented on the above drawing shows a unit price for concrete of $156 per cubic yard which is considerably below the unit costs reported for other concrete work in the locale.

3. An accepted rule of thumb for the design of large telescopes is that the mass of the stationary elements of the telescope, its pier and foundation should be approximately five times the mass of the moving elements of the telescope. This should be checked.

4. The section shown on the above drawing, and the foundation plans prepared by A. Y. Yee, show an undesirable closeness of the dome footings to both the telescope and the spectrograph foundations.

5. The A. Y. Yee drawing of the foundation plan does not show tie beams between the dome footings. The structural engineer should substantiate their omission.

D. General Comments

1. More complete data on wind velocities is needed.

2. Dead and live loads are needed.

3. Permissible settlements, differential settlements and tilts are needed.

4. Establish a maximum operating wind velocity and permissible telescope foundation tilts at that wind velocity.

5. The minimum natural frequency for the telescope, pier and footing system should be specified. Our preliminary calculations for the natural frequency of the telescope, pier and footing in a vertical axis indicate it will be on the order of 4 Hz.

AAR:ch

cc: R. D. Casperson
F. W. Stoller